

Communication

Inhibitory effect and mechanism of chitosan–Ag complex hydrogel on fungal disease in Grape

Weizhong He ^{1,2}, Yajuan Zhu ^{3,*}, Yan Chen ⁴, Qi Shen ^{1,2}, Zhenyu Hua ^{1,2}, Xian Wang ^{1,2} and Peng Xue ^{1,2,*}

¹ Institute of Quality Standards & Testing Technology for Agro-Products, Xinjiang Academy of Agricultural Sciences, Urumqi 830091, China; hewei198112@126.com (W.H.); shenqi068@163.com (Q.S.); huakobe@163.com (Z.H.); wangxian_707@163.com (X.W.)

² Key Laboratory of Agro-Product Quality and Safety of Xinjiang, Laboratory of Quality and Safety Risk Assessment for Agro-Products (Urumqi), Ministry of Agriculture and Rural Affairs, Urumqi 830091, China

³ The Center for Disease Control and Prevention of Xinjiang Production and Construction Crops, Urumqi, Xinjiang 830002, China

⁴ Engineering Research Center of Clinical Functional Materials and Diagnosis & Treatment Devices of Zhejiang Province, Wenzhou Institute, University of Chinese Academy of Sciences (Wenzhou Institute of Biomaterials & Engineering), Wenzhou 325000, China; chenyan20@ucas.ac.cn (Y. C.)

* Correspondence: zhuyajuan1988@126.com (Y.Z.); xuepeng416@126.com (P.X.)

Abstract: Hydrogel antibacterial agent is an ideal antibacterial material because of it could diffuses antibacterial molecules into the decayed area by providing a suitable microenvironment and the hydrogel acts as a protective barrier on the decay interface. The biocompatibility and biodegradation make the removal process easily which were widely used in medical fields. However, there have been few reports on its application for controlling postharvest diseases in fruit. In this study, the Chitosan-Ag (CS-Ag) complex hydrogels were prepared using the physical crosslinking method, which used for controlling postharvest diseases in grape. The prepared hydrogels were stable for a long period at room temperature. The structure and surface morphology of CS-Ag composite hydrogels were characterized by UV-Vis, FTIR, SEM, and XRD. The inhibitory effects of CS-Ag hydrogel on disease in grape caused by *P. expansum*, *A. niger* and *B. cinerea* were investigated both in vivo and in vitro. The remarkable antibacterial activity of CS-Ag hydrogels was mainly due to the synergistic antibacterial and antioxidant effects of CS and Ag. Preservation test showed that the CS-Ag hydrogel had positive fresh-keeping effect. This revealed CS-Ag hydrogels plays a critical role in controlling fungal disease in grape.

Keywords: silver; chitosan; hydrogel; antibacterial; grape

1. Introduction

The decay process of fruit is caused by a series of microorganisms infection and reproduction [1]. *Aspergillus* and *Penicillium* produce toxic secondary metabolites

during postharvest of grape, which posing to a high risk of disease for consumers and demand for natural, green and safety antibacterial agent for the preservation of grapes is growing [3]. Hydrogel antibacterial agent is the synthetic or natural biological material, which is an ideal antibacterial material [4,5]. It diffuses antibacterial molecules into the decayed area by providing a suitable microenvironment, and acts as a protective barrier at the decay interface [6]. The biocompatibility, biodegradation and self-healing properties make the removal process easily, and which were widely used in medical and agriculture [7-9].

Hydrogels based on chitosan (CS) have attracted considerable interest and have been widely used as antibacterial agents because of their non-toxic, biocompatible, renewable and biodegradable features [10-12]. The broad-spectrum antibacterial activity of chitosan is related to its physical and chemical properties, and is restricted by the types of microorganisms [13]. The antibacterial properties can be significantly increased when the

CS blended with silver ion (Ag^+) or silver nanoparticles (AgNPs) [14]. However, the AgNPs are easy to agglomerate and oxidize exposed to air, which affects antibacterial performance. In addition, the application may also cause damage to human liver [15]. One particular solution is to prevent the self-aggregation of Ag particles by embedding Ag composites into hydrogels frameworks [16,17]. Although a few antibacterial Chitosan-silver (CS-Ag) conjugates materials have been reported, none of them are commercially available and most are used in medical and pharmaceutical field rather than in agriculture [18].

In this communication, the CS-Ag hydrogels were prepared using the physical crosslinking method and characterized by UV-Vis, FTIR, SEM, and XRD. The inhibitory effect of CS-Ag gel against the fungal species during grape storage were investigated both in vitro and in vivo. Preservation test showed that the CS-Ag hydrogel had positive fresh-keeping effect. Furthermore, the inhibitory effect of CS-Ag complex gel on fungi and the underlying mechanism of CS-Ag gel against the fungi were explored.

2. Results and Discussion

2.1. Fungal identification

Three fungal species were identified as *Penicillium expansum* (*P. expansum*), *Aspergillus niger* (*A. niger*) and *Botrytis cinerea* (*B. cinerea*) by Morphological and molecular identification. (Supplementary Materials, Figure S1 and Figure S2.)

2.2. CS-Ag hydrogel

CS-Ag hydrogel had excellent gelation properties. The scanning electron microscopy (SEM) of the morphology of the CS-Ag hydrogel (Figure 1) revealed that the CS-Ag sample was composed of interconnected nanostructures, whereas the CS alone was much smoother (Supplementary Material Figure S3), indicating that the interwoven networks were cross-linked by Ag^+ ions [19].

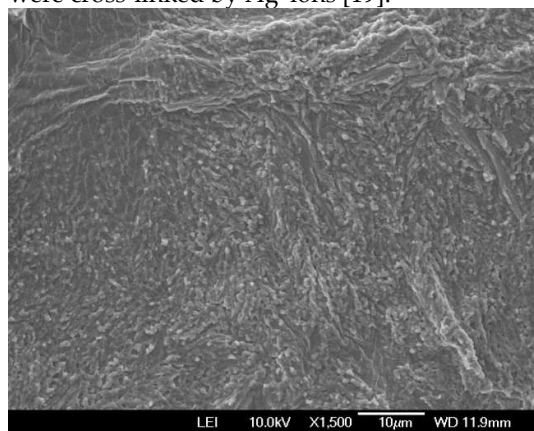


Figure 1. SEM image of the CS-Ag hydrogel.

The Ag^+ ions in the complexation with CS were proved by concentration-dependent UV-Vis absorption spectra (Figure 2). The CS solution transformed into a hydrogel when the Ag^+ solution gradual introduction. The intensity of the absorbance increased significantly with increasing Ag^+ ion concentration, with the maximum absorption band undergoing a red shift from $\lambda = 287 \text{ nm}$ to 298 nm . This result was attributed to the coordination of the Ag^+ ions, having empty orbitals, to the CS chains, which have plenty of free hydroxy and amino groups with abundant lone-pair electrons [20]. The time-dependent UV-Vis absorption spectrum (Figure 3) indicating that the process is not time dependent, which can be ascribed to the extremely fast complexation between the Ag^+ ions and the CS polymer chains.

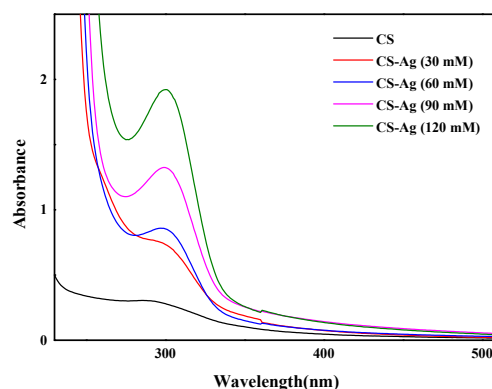


Figure 2. The concentration-dependent UV-Vis absorption spectra of CS-Ag hydrogel.

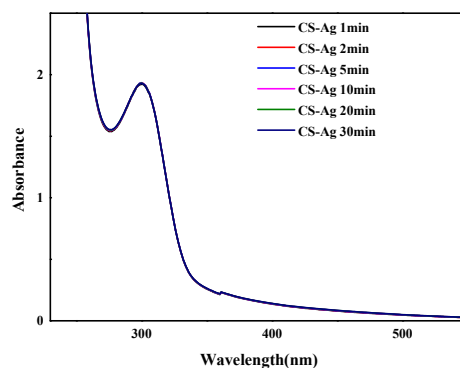


Figure 3. The time-dependent UV-Vis absorption spectra of CS-Ag hydrogel.

The FTIR spectra of the CS powders and the CS-Ag xerogels were confirmed the complexation of CS and Ag^+ . The major evidence for the interaction of CS and Ag^+ ions is the shift of the band at 3450 cm^{-1} (attributable to CS νOH and νNH absorptions) to 3420 cm^{-1} (Figure 4) [20]. Furthermore, from CS to CS-Ag xerogel the amide II band at 1600 cm^{-1} underwent a blue shift and the C-N band at 1400 cm^{-1} a red shift. These shifts revealed that both $-\text{OH}$ and $-\text{NH}_2$ groups in the CS chains took part in the coordination complexation which promoted the rapid gel-network formation [21].

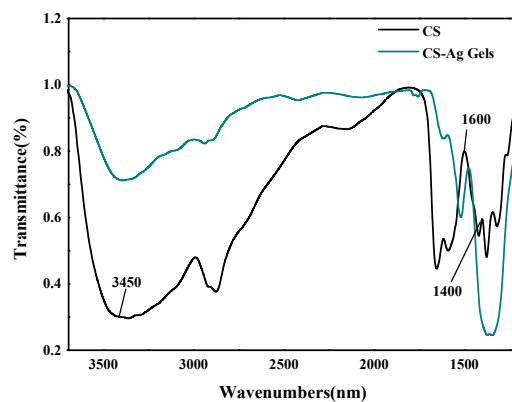


Figure 4. FTIR spectra of CS powders and CS-Ag xerogels.

The XRD patterns of the CS-Ag xerogel (Figure 5), the intensity of the peak at $2\theta = 20^\circ$ for the crystal form of the pure CS powders decreased significantly and only a much broader, less intense peak at $2\theta = 30^\circ$ was detected for the CS-Ag xerogels. This change in the XRD spectrum is as a result of the complexation between the Ag^+ ions and the CS chains through -OH and - NH_2 binding sites, thus efficiently reducing the hydrogen bonding and destroying the crystal structure of the CS chains [21]. These results were in agreement with the UV-Vis and FTIR.

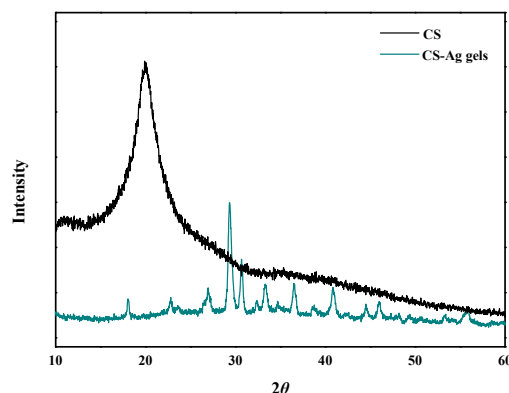


Figure 5. XRD pattern of the CS powders and CS-Ag xerogels.

2.3. Inhibition of CS-Ag complex hydrogel on fungi disease in vitro

The antibacterial results of CS-Ag gel and CS-AgNPs hybrid sol on *P. expansum*, *A. niger* and *B. cinerea* were shown in Figure 6. CS-Ag gel revealed a remarkable inhibitory effect on all tested fungi. In the absence of CS-Ag gel, colonies expanded over time. Compared with the CK groups, *P. expansum*, *A. niger* and *B. cinerea* could not grow and reproduced on CS, however CS had no obvious inhibitory effect on these. Ag^+ had a certain inhibitory effect on three fungi, which was slightly inferior than AgNPs. The antibacterial effect of CS-AgNPs sol on *P. expansum*, *A. niger* and *B. cinerea* were similar to that of AgNPs. CS-Ag hydrogel showed obvious antibacterial area to all tested fungi.

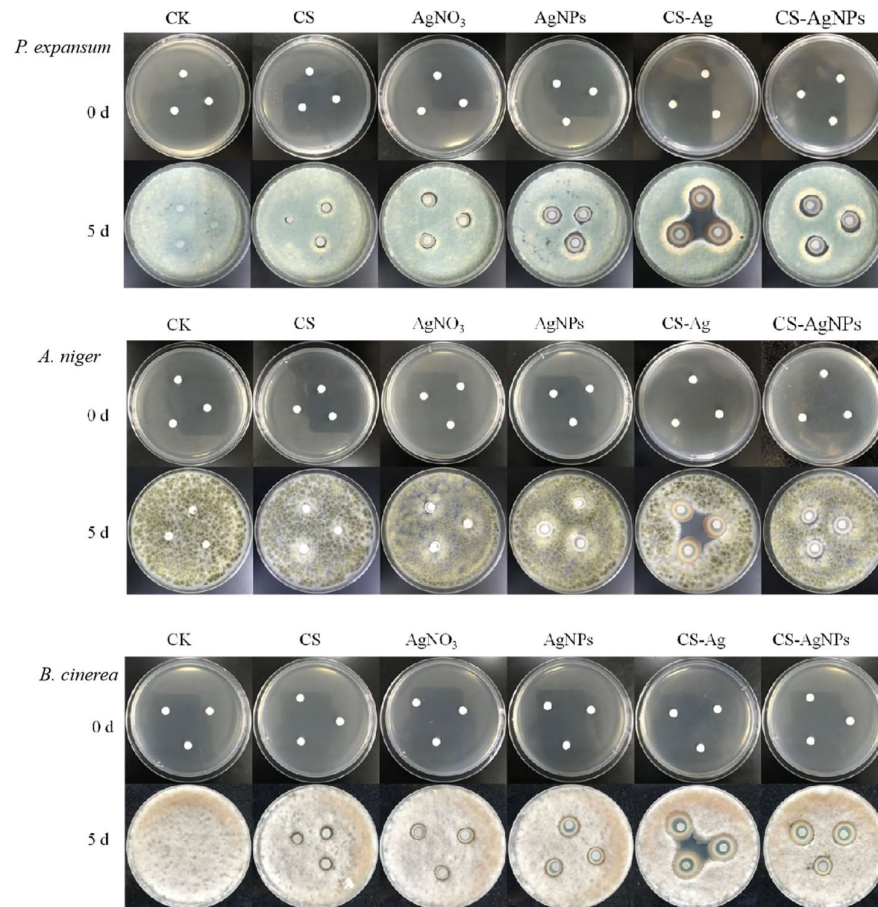


Figure 6. The antibacterial effect of different concentrations of CS-Ag xerogels bacteriostatic agent on colony growth of *P. expansum*, *A. niger* and *B. cinerea*. (0.62 wt% CS-Ag hydrogel, CS 1.7 mg·mL⁻¹, Ag⁺ 4.5 mg·mL⁻¹; 0.62 wt% CS-AgNPs sol, CS 1.7 mg·mL⁻¹, AgNPs 4.5 mg·mL⁻¹; CS 1.7 mg·mL⁻¹; AgNO₃ 4.5 mg·mL⁻¹; AgNPs 4.5 mg·mL⁻¹)

2.4. Impact of CS-Ag hydrogel on grape disease in vivo

The different concentrations of CS-Ag gel antibacterial agents (0.1, 0.2, 0.4, 0.5 wt%) were selected to treat grapes that had been inoculated with fungi (Figure 7). The results show that inverse correlation was found between fungal growth and CS-Ag hydrogel concentration. CS-Ag gel can significantly inhibit the fungal diseases caused by *P. expansum*, *A. niger* and *B. cinerea*. CS-Ag gel could delay the onset of grapes, reduce the severity of grape diseases and grape decay index. The CK samples which spraying suspension of *P. expansum*, *A. niger* and *B. cinerea*. had begun to decay at 48 h. Although 0.1% CS-Ag gel agent treatment group have shown rotten, the decay index was significantly lower than that of CK group. The experimental data expressed that 0.4% CS-Ag gel agent has obvious inhibitory effect on *P. expansum* and *B. cinerea*., and 0.2% CS-Ag gel could inhibit on *A. niger*. The occurrence of fungal diseases in grape were completely controlled within 72 h, and the disease index was 0. Compared with CK group, the decay index of *P. expansum*, *A. niger* and *B. cinerea*. disease decreased by 100%, 96.34% and 100% respectively.

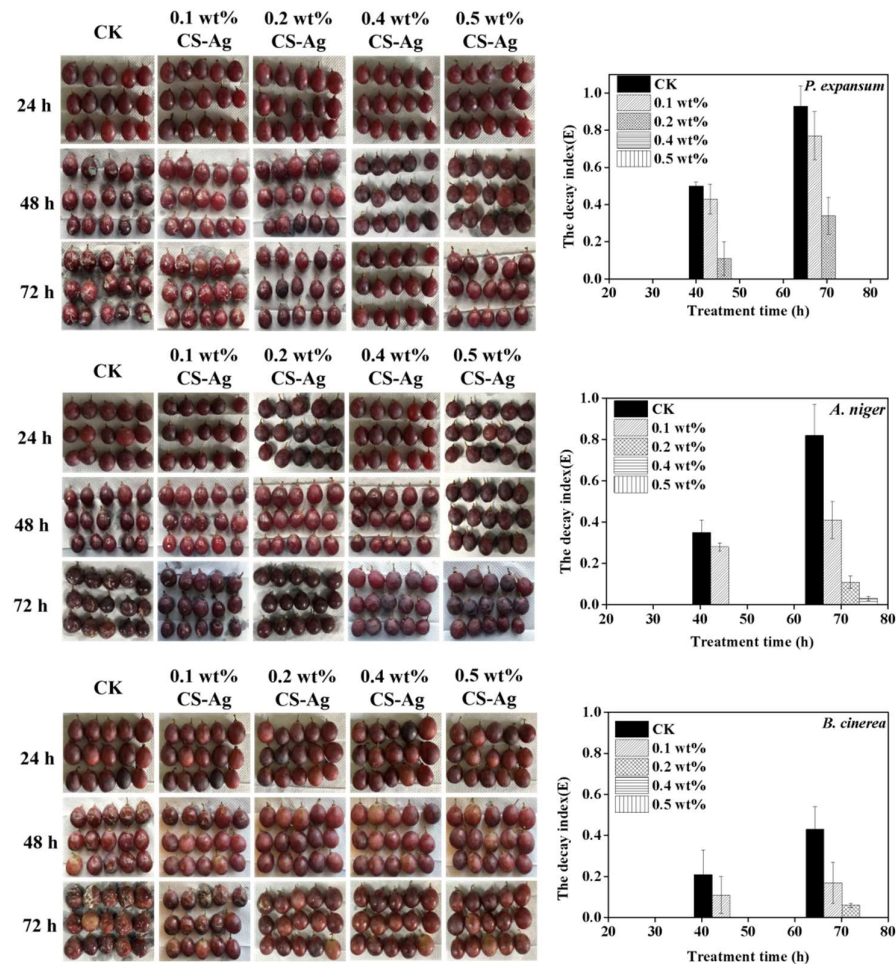


Figure 7. Antibacterial effect of CS-Ag gels bacteriostatic agent on fungal disease caused by *P. expansum*, *A. niger* and *B. cinerea* in grape. Vertical bars represented standard deviations of the means.

In order to investigate the effects of CS on grape preservation, the grapes were treated with different concentrations of CS-Ag gel and stored at room temperature for 40 days. The decay rate and weight loss rate of grape greatly affect its commercial value and edible taste. An inverse correlation was found between decay rate and CS-Ag gel concentration (Supplementary Materials, Figure S6). As the increase of time, the weight loss rate of CK group was significantly higher than other groups and 0.5% CS-Ag gel agent and 0.5% CS solution were lower than others (Supplementary Materials, Figure S7). This may indicate that CS treatment is easy to form a film on the fruit surface, which increase the peel thickness and block part of the peel pores. To some extent, it can reduce the transpiration of water in grape and maintain the water [9,14]. The experiment of total soluble solid (TSS), titratable acid and vitamin C content indicated that 0.2 wt% CS-Ag gel treatment could delay the decrease the nutrient loss in fruit, and maintaining the content of grape physiological quality at a certain level. (Supplementary Materials, Figure S8-S10.)

In conclusion, CS-Ag gel agent can not only control grape fungal diseases well, but also preserve grape storage quality.

2.5. Effect of CS-Ag on fungal morphology

The scanning electron microscopy (SEM) to obtain a direct view of the morphology of fung. As shown in Figure 8, the SEM image revealed that the treatment with CS-Ag gel antibacterial agent had a great influence on the morphology of cell wall of conidia such as *P. expansum*, *A. niger* and *B. cinerea*, and the structure of cell wall was damaged by folds or

even broken, resulting in the leakage of cell protoplasm. Integrated with the literature has to report for duty, the destruction of the structure of the fungus by the CS-Ag gel antibacterial agent may be caused by the synergistic effect of CS and Ag^+ [13]. Both chitosan and Ag^+ with a positive charge, which can interact with pathogen negative charge on the surface of the cell membrane and change the permeability of cell membrane that could cause cell material leakage and reduce the cell activity which lead to cell membranes and fungal DNA damage [22,23].

CS-Ag hydrogel changes the morphology of mycelia and destroys the integrity of cell membrane, which may affect the permeability of plasma membrane leading to imbalance of intracellular osmotic pressure and leakage of cytoplasmic contents [24,25]. Moreover, the hydroxyl groups in antibacterial compounds can form hydrogen bonds with active enzymes, resulting in deactivation and blocked enzymatic reactions, these may lead to cell necrosis and inhibit the growth and reproduction of fungi to control grape mycosis. These synergistic effect of CS and Ag^+ can probably lead to cell necrosis easily [26].

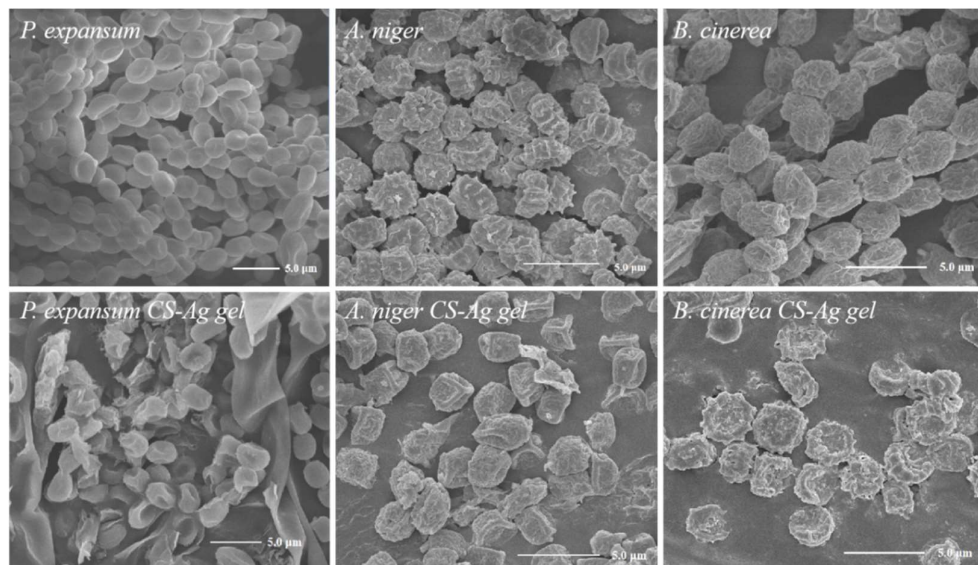


Figure 8. Effect of CS-Ag on surface microstructure of *P. expansum*, *A. niger* and *B. cinerea*.

3. Materials and Methods

3.1. Fruit Material and Chemical Material

Grape (Midnight Beauty) were purchased from Tulufan, Xinjiang, China. All fruits were free from mechanical damage or infection. The surface of the selected fruits was disinfected with 75% ethanol for 5 min, washed twice with sterile water and air-dried.

Low molecular weight chitosan (85% deacetylated) and agar powder (bacteriological grade) were procured from Sigma-Aldrich, USA. Silver nitrate (AgNO_3 , 99.8%; Energy), acetic acid (glacial, 99 100%; Sinopharm), sodium citrate (95%; Sinopharm) and sodium hydroxide (NaOH , Sinopharm) 4-nitrophenol (95%; Merck) were used as received without further purification. All other chemicals used in this study were of analytical grade.

3.2. Fungal isolation, identification, culture and spore suspension

The procedure refers to previous literature [27]. The decayed grape was washed with sterile water, the filtrate was collected and diluted, and then 100 μL diluted solution was uniformly spread on a petri dish containing potato dextrose agar (PDA) medium and cultured at 28 $^{\circ}\text{C}$ for 7 d. The fungal isolates were purified three times on PDA.

The major isolates were obtained and characterized using macroscopic and microscopic observation methods. Le Lay's method was used for genotyping (2016), and the

obtained sequences were subjected to a comparison with the GenBank database using the Basic Local Alignment Search Tool (BLAST; <http://www.ncbi.nlm.nih.gov/BLAST>).

The isolated fungi were separately cultured on PDA at 28 °C for 7 d. Spore suspensions were obtained by rinsing the cultures with sterile water containing 0.05% (v/v) Tween-80 and then adjusted to 1×10^9 CFU/L.

3.3. Characterization

UV-Vis spectrum was recorded on Shimadzu UV-2550 spectrometer (Japan). Fourier transform infrared spectroscopy (FT-IR) was carried out in Bruker EQUINOX-55 (Germany). X-ray diffraction (XRD) was carried out using Bruker D8 Advance (Germany). Scanning electron microscopy (SEM) images were obtained from the field emission SEM (SU8010, Hitachi, Japan). Transmission electron microscopy (TEM) was taken using Hitachi H-600 (Japan).

3.4. Preparation of CS-Ag hydrogel and CS-AgNPs sol

Chitosan-Ag Hydrogel. The 1 mL CS-Ag hydrogel was prepared by adding 100 μ L 0.2 M NaOH to 800 μ L 0.5 wt % CS solution (in 1 % acetic acid), followed by adding 100 μ L freshly prepared 0.3 M AgNO₃ solution with vigorous shaking for 2 seconds. The Critical Gelation Concentration (CGC) of the hydrogel was visually recognized by the reversed vial test method (Supplementary Materials, Figure S4).

Chitosan-AgNPs Sol. The 0.3 M AgNPs sol was prepared by adding 10 mL 3.0 M AgNO₃ to 80 mL water, followed by adding 10 mL 3.0 M sodium citrate standard solution with vigorous shaking, and heated in the microwave oven for 3 min. The 1 mL CS-AgNPs Sol was prepared by adding 100 μ L 0.2 M NaOH to 800 μ L 0.5 wt % CS solution (in 1 % acetic acid), followed by adding 100 μ L 0.3 M AgNPs sol with vigorous shaking. The morphology of AgNPs was observed by TEM (Supplementary Materials, Figure S5).

3.5. Inhibitory effect of CS-Ag hydrogel on fungi in vitro

All experimental operations are carried out in a clean workbench.

3.5.1. Preparation of fungal suspension

Pick up 3 needles of pathogenic fungi strains into the test tube containing 10 mL sterile water, and then shake the test tube well to make 10^{-1} fungi suspension.

3.5.2. Antibacterial experimental method

Preparation of bacteriostatic tablets: Prepare the qualitative filter paper into a circular paper with a diameter of 6 mm with a punch, then put these filter paper into an autoclave at 121 °C for 20 min, then dry for later use. Immerse the sterilized and dried 6 mm filter paper disc into different bacteriostatic solutions.

Fungal inoculation: inoculate 500 μ L fungal suspension on the culture medium, mix evenly, then cover the petri dish and dry it at room temperature for 5 min.

Put the filter paper that treated with antibacterial agent gently on the medium coated with bacteria by using sterilized tweezers, and put 3 pieces on each medium. The distance between the centers of each filter paper is more than 30 mm, and the distance from the edge of the petri dish is more than 20 mm. The filter paper was tightly attached to the medium, covered the petri dish was and placed at 28 °C for 5 d observation

After pasting the filter paper, gently press the filter paper with tweezers to make it tightly adhere to the culture medium and cover the culture dish, Place it in a 28°C incubator and culture for 5 days. Measure the diameter of the bacteriostatic circle with a vernier caliper and record the results.

3.6. Control of CS-Ag hydrogel on fungal disease in vivo

In order to ensure the pathogenicity, the grapes were uniformly sprayed with suspensions of the tested fungal spores and dried. The grapes were soaked in CS-Ag hydrogel at different concentrations, and then placed in a sealing bag. All samples were cultured at $20 \pm 2^\circ\text{C}$ and $70 \pm 10\%$ relative humidity in the incubator. Surface decay on

the grapes was recorded on a regular basis. All treatments were performed in triplicate and the entire experiment was repeated two times.

The decay index (E) was calculated by scoring the total decayed area on each fruit surface: class 0, no visible decay; class 1, decay accounts for less than 25% of the surface area; class 2, decay accounts for 25–50% of the surface area; class 3, decay accounts for 50–75% of the surface area; and class 4, decay accounts for more than 75% of the surface area. The decay index (E) was calculated using the following formula:

$$\text{The decay index (E)} = \frac{\sum(\text{the number of decayed fruits in each class} \times \text{decay scale})}{\text{the total number of treated fruits} \times \text{the decay scale}}$$

3.7 Preservation Test of CS-Ag hydrogel

The fresh grapes were divided into seven parts and separately soaked in 0.5% Chitosan, 0.1% CS-Ag Hydrogel, 0.2% CS-Ag Hydrogel, 0.4% CS-Ag Hydrogel, 0.5% CS-Ag Hydrogel, CK group with no processing. The soaked grapes were sampled regularly at room temperature (temperature 20 ± 2.0 °C, relative humidity $20 \pm 5\%$), the storage quality was evaluated by determining the weight loss rate, decay rate, soluble solids, titratable acid and vitamin C content. All indicators were determined, and each treatment was repeated three times. The vertical bar represents the standard deviation of the mean.

The decay rates.

$$\text{The decay rate} = \frac{\text{the weight of decay grape}}{\text{the weight of grape}} \times 100\%$$

Weight loss rate. The weight of grapes was weighed by weighing method before and after storage, and the weight loss rate was calculated.

$$\text{Weight loss rate} = \frac{\text{the weight difference of grape before and after storage}}{\text{the weight of grape before storage}} \times 100\%$$

Total soluble solid. The method of refractometer in NY/T 2637-2014 was used to determine the content of soluble solids in grape by using a hand-held digital refractometer.

Titratable acid content (TSS). The acid-base titration method was used. Take appropriate number of grapes, homogenate, and add 30 mL distilled water into triangle bottle. water bath for 30 min, cool and filter. 10 mL filtrate was added with phenolphthalein indicator and titrated to micro red with sodium hydroxide solution.

Vitamin C content. The method of 2,6-dichloroindophenol titration in GB5009.86-2016 was used to determine vitamin C content.

3.8. Morphology of fungal

The analyze of differences in the micro-morphological structures between the CS-Ag and CK groups for the tested fungi were examined using a scanning electron microscope. For that a 10 µL drop of each sample was deposited on a silicon slide, dried and sputter-coated with gold film in a sputter coater.

4. Conclusions

In summary, the results of both in vitro and in vivo studies indicate CS-Ag hydrogel effectively controls disease in grape, strongly inhibits the growth of *P. expansum*, *A. niger* and *B. cinerea*. The antibacterial performance of CS-Ag complex is improved because of the synergistic effect of both CS and Ag. Meanwhile, it also has remarkable preservation effect. The use of CS-Ag complex hydrogel can not only improve food safety by eliminating fungal spread but also leave no detectable residues after simple water washing. CS-Ag complex hydrogel improves grape safety and can be used as an alternative fungistat agent for fruit to control fungal disease.

Supplementary Materials: The following are available online, Figure S1: Figure S1. The image of dominant pathogenic fungi isolated from grape. (a: *P. expansum*, b: *A. niger* and c: *B. cinerea*.), Figure S2: Identification of dominant pathogenic fungi isolated from grape.(a: *P. expansum*, b: *A. niger*

and c: *B. cinerea*.), Figure S3: SEM image of the CS gel, Figure S4: The CGC of CS-Ag complex hydrogel, Figure S5: TEM image of AgNPs, Figure S6: CS-Ag hydrogel effect on decay rate of grape during postharvest, Figure S7: CS-Ag hydrogel effect on weight loss rate of grape during postharvest, Figure S8: CS-Ag hydrogel effect on soluble solids of grape during postharvest, Figure S9: CS-Ag hydrogel effect on titratable acids of grape during postharvest, Figure S10: CS-Ag hydrogel effect on Vitamin C of grape during postharvest.

Author Contributions: W. H. and Y. Z. contributed equally; Conceptualization, Y. Z., Y. C. and P. X.; investigation, Y.Z.; writing—original draft preparation, W. H. and P. X.; data curation, Q. S., Z. H. and X. W.; writing—review and editing, W. H., Y.Z. and P. X.; All authors have read and agreed to the published version of the manuscript.

Funding: This work was supported by the Key Laboratory of Xinjiang Uygur Autonomous Region Open Project (No. 2017D04015.).

Data Availability Statement: The data presented in this study are available on request from the corresponding author.

Acknowledgments: The authors thank the Project of Renovation Capacity Building for the Young Sci-Tech Talents Sponsored by Xinjiang Academy of Agricultural Sciences (No. xjnkq-2019015) and Dr. Tianchi Program of the Autonomous Region.

Conflicts of Interest: The authors declare no conflict of interest.

Sample Availability: Samples of the compounds are available from the authors.

References

1. Sanzani, S. M.; Reverberi, M.; Geisen, R. Mycotoxins in harvested fruits and vegetables: Insights in producing fungi, biological role, conducive conditions, and tools to manage postharvest contamination. *Postharvest Biol. Tec.* **2016**, *122*, 95-105.
2. Alkan, N.; Fortes, A. M. Insights into molecular and metabolic events associated with fruit response to post-harvest fungal pathogens. *Front. Plant. Sci.* **2015**, *6*, 889. doi:10.3389/fpls.2015.00889
3. Chouhan, D.; Mandal, P. Applications of chitosan and chitosan based metallic nanoparticles in agrosociences-A review. *Int. J. Biol. Macromol.* **2021**, *166*, 1554-1569.
4. Zhang, M.; Wang, G.; Wang, D.; Zheng, Y.; Li, Y.; Meng, W.; Zhang, X.; Du, F.; Lee, S. Ag@MOF-loaded chitosan nanoparticle and polyvinyl alcohol/sodium alginate/chitosan bilayer dressing for wound healing applications. *Int. J. Biol. Macromol.* **2021**, *175*, 481-494.
5. Zheng, J.; Fan, R.; Wu, H.; Yao, H.; Yan, Y.; Liu, J.; Ran, L.; Sun, Z.; Yi, L.; Dang, L.; Gan, P.; Zheng, P.; Yang, T.; Zhang, Y.; Tang, T.; Wang, Y. Directed self-assembly of herbal small molecules into sustained release hydrogels for treating neural inflammation. *Nat. Commun.* **2019**, *10*, 1604. doi:10.1038/s41467-019-09601-3
6. Shafique, M.; Sohail, M.; Minhas, M. U.; Khaliq, T.; Kousar, M.; Khan, S.; Hussain, Z.; Mahmood, A.; Abbasi, M.; Aziz, H. C.; Shah, S. A. Bio-functional hydrogel membranes loaded with chitosan nanoparticles for accelerated wound healing. *Int. J. Biol. Macromol.* **2021**, *170*, 207-221.
7. Xu, H.; Zhang, L.; Zhang, H.; Luo, J.; Gao, X. Green Fabrication of Chitin/Chitosan Composite Hydrogels and Their Potential Applications. *Macromol. Biosci.* **2021**, *21*, 2000389. doi:10.1002/mabi.202000389
8. Yang, J.; Shen, M.; Luo, Y.; Wu, T.; Wen, H.; Xie, J. Construction and characterization of Mesona chinensis polysaccharide-chitosan hydrogels, role of chitosan deacetylation degree. *Carbohydr. Polym.* **2021**, *257*, 117608. doi:10.1016/j.carbpol.2020.117608
9. Ehtesham Nia, A.; Taghipour, S.; Siahmansour, S. Pre-harvest application of chitosan and postharvest Aloe vera gel coating enhances quality of table grape (*Vitis vinifera* L. cv. 'Yaghouti') during postharvest period. *Food Chem.* **2021**, *347*, 129012. doi:10.1016/j.foodchem.2021.129012
10. Mejdoub-Trabelsi, B.; Touihri, S.; Ammar, N.; Riahi, A.; Daami-Remadi, M. Effect of chitosan for the control of potato diseases caused by Fusarium species. *J. Phytopathol.* **2020**, *168*, 18-27.

11. González-Reza, R. M.; Hernández-Sánchez, H.; Quintanar-Guerrero, D.; Alamilla-Beltrán, L.; Cruz-Narváez, Y.; Zambra-no-Zaragoza, M. L. Synthesis, Controlled Release, and Stability on Storage of Chitosan-Thyme Essential Oil Nanocapsules for Food Applications. *Gels* **2021**, *7*, 212. doi:10.3390/gels7040212
12. Muñoz, Z.; Moret, A.; Garcés, S. Assessment of chitosan for inhibition of *Colletotrichum* sp. on tomatoes and grapes. *Crop. Prot.* **2009**, *28*, 36-40.
13. Ashrafi, M.; Bayat, M.; Mortazavi, P.; Hashemi, S. J.; Meimandipour, A. Antimicrobial effect of chitosan-silver-copper nanocomposite on *Candida albicans*. *J. Nanostructure Chem.* **2020**, *10*, 87-95.
14. Polinarski, M. A.; Beal, A. L. B.; Silva, F. E. B.; Bernardi-Wenzel, J.; Burin, G. R. M.; de Muniz, G. I. B.; Alves, H. J. New Perspectives of Using Chitosan, Silver, and Chitosan-Silver Nanoparticles against Multidrug-Resistant Bacteria. *Part. Part. Syst. Char.* **2021**, *38*, 2100009. doi:10.1002/ppsc.202100009
15. Kim, Y. S.; Song, M. Y.; Park, J. D.; Song, K. S.; Ryu, H. R.; Chung, Y. H.; Chang, H. K.; Lee, J. H.; Oh, K. H.; Kelman, B. J.; Hwang, I. K.; Yu, I. J. Subchronic oral toxicity of silver nanoparticles. *Part. Fibre Toxicol.* **2010**, *7*, 20. doi:10.1186/1743-8977-7-20
16. Kozicki, M.; Kołodziejczyk, M.; Szykowska, M.; Pawlaczyk, A.; Leśniewska, E.; Matusiak, A.; Adamus, A.; Karolczak, A. Hydrogels made from chitosan and silver nitrate. *Carbohydr. Polym.* **2016**, *140*, 74-87.
17. Zhang, Z.; He, T.; Yuan, M.; Shen, R.; Deng, L.; Yi, L.; Sun, Z.; Zhang, Y. The in situ synthesis of Ag/amino acid biopolymer hydrogels as mouldable wound dressings. *Chem. Commun.* **2015**, *51*, 15862-15865.
18. Kim, J. S.; Kuk, E.; Yu, K. N.; Kim, J.-H.; Park, S. J.; Lee, H. J.; Kim, S. H.; Park, Y. K.; Park, Y. H.; Hwang, C.-Y.; Kim, Y.-K.; Lee, Y.-S.; Jeong, D. H.; Cho, M.-H. Antimicrobial effects of silver nanoparticles. *Nanomed-Nanotechnol.* **2007**, *3*, 95-101.
19. Sun, Z.; Lv, F.; Cao, L.; Liu, L.; Zhang, Y.; Lu, Z. Multistimuli-Responsive, Moldable Supramolecular Hydrogels Cross-Linked by Ultrafast Complexation of Metal Ions and Biopolymers. *Angew. Chem. Int. Ed.* **2015**, *54*, 7944-7948.
20. Hernández, R. B.; Franco, A. P.; Yola, O. R.; López-Delgado, A.; Felcman, J.; Recio, M. A. L.; Mercê, A. L. R. Coordination study of chitosan and Fe³⁺. *J. Mol. Struct.* **2008**, *877*, 89-99.
21. Qu, J.; Hu, Q.; Shen, K.; Zhang, K.; Li, Y.; Li, H.; Zhang, Q.; Wang, J.; Quan, W. The preparation and characterization of chitosan rods modified with Fe³⁺ by a chelation mechanism. *Carbohydr. Res.* **2011**, *346*, 822-827.
22. Biao, L.; Tan, S.; Wang, Y.; Guo, X.; Fu, Y.; Xu, F.; Zu, Y.; Liu, Z. Synthesis, characterization and antibacterial study on the chitosan-functionalized Ag nanoparticles. *Mat. Sci. Eng. C* **2017**, *76*, 73-80.
23. Wakshlak, R. B.; Pedahzur, R.; Avnir, D. Antibacterial activity of silver-killed bacteria: the "zombies" effect. *Sci. Rep.* **2015**, *5*, 9555. doi:10.1038/srep09555
24. Nakamura, C. V.; Ishida, K.; Faccin, L. C.; Filho, B. P. D.; Cortez, D. A. c. G.; Rozental, S.; de Souza, W.; Ueda-Nakamura, T. In vitro activity of essential oil from *Ocimum gratissimum* L. against four *Candida* species. *Res. Microbiol.* **2004**, *155*, 579-586.
25. Boxi, S. S.; Mukherjee, K.; Paria, S. Ag doped hollow TiO₂ nanoparticles as an effective green fungicide against *Fusarium solani* and *Venturia inaequalis* phytopathogens. *Nanotechnology* **2016**, *27*, 085103. doi:10.1088/0957-4484/27/8/085103
26. Tian, J.; Ban, X.; Zeng, H.; Huang, B.; He, J.; Wang, Y. In vitro and in vivo activity of essential oil from dill (*Anethum graveolens* L.) against fungal spoilage of cherry tomatoes. *Food Control* **2011**, *22*, 1992-1999.
27. Chen, Y.; Guo, Q.; Wei, J.; Zhang, J.; Zhang, Z.; Wang, J.-d.; Wu, B. Inhibitory effect and mechanism of nitric oxide (NO) fumigation on fungal disease in Xinjiang Saimaiti dried apricots. *LWT-Food Sci. Technol.* **2019**, *116*, 108507. doi:10.1016/j.lwt.2019.108507